Palladium(II) complexes of OS donor N-(di(butyl/ phenyl) carbamothioyl) benzamide and their antiamoebic activity

ARTICLE *in* EUROPEAN JOURNAL OF MEDICINAL CHEMISTRY · MAY 2015

Impact Factor: 3.45 · DOI: 10.1016/j.ejmech.2015.05.006

European Journal of Medicinal Chemistry 98 (2015) 54–60

Contents lists available at ScienceDirect

European Journal of Medicinal Chemistry

journal homepage: http://www.elsevier.com/locate/ejmech

Short communication

Palladium(II) complexes of OS donor N-(di(butyl/phenyl) carbamothioyl)benzamide and their antiamoebic activity

Mannar R. Maurya [a, *], Bhawna Uprety [a], Fernando Avecilla [b], Saba Tariq [c], Amir Azam [c]

[a] Department of Chemistry, Indian Institute of Technology Roorkee, Roorkee 247667, India
[b] Departamento de Química Fundamental, Universidade da Coruña, Campus de A Zapateira, 15071 A Coruña, Spain
[c] Department of Chemistry, Jamia Millia Islamia, Jamia Nagar, New Delhi 100 025, India

ARTICLE INFO

Article history:
Received 16 September 2014
Received in revised form
3 May 2015
Accepted 4 May 2015
Available online 7 May 2015

Keywords:
Palladium complexes
NMR spectra
OS donor ligands
Crystal structure
Antiamoebic activity

ABSTRACT

Two promising palladium(II) compounds of general formula, *cis*–[*Pd*(*L*-*O*,*S*)$_2$] [where HL-O,S = N-(di(butyl/phenyl)carbamothioyl)benzamide] as metal based antiamoebic drug candidates, have been synthesized. Both complexes are characterized in the solid state by FT-IR spectroscopy, TGA and single crystal X-ray study, as well as in solution by other spectroscopic techniques such as ^{1}H and ^{13}C NMR, and UV–visible. All these studies confirm the coordination of ligands through oxygen and sulphur atoms upon thioenolization induced delocalization. Complexes adopt *cis*-configuration in the solid state. Both the complexes and their respective ligands were screened *in vitro* for antiamoebic activity against *HM1:1MSS* strain of *Entamoeba histolytica* by microdilution method and cell viability in response to drugs was checked by using MTT assay. The IC_{50} values in the range 0.30–0.80 μM for ligands as well as complexes compared to 1.40 for metronidazole along with their similar inhibitory effect on cell viability of HEK293 cells like metronidazole make them promising future antiamoebic drugs.

1. Introduction

Amoebiasis is an infection of the human gut caused by the protozoan parasite *Entamoeba histolytica.* It is responsible for 100,000 fatalities per annum [1]. Untreated infection may lead to serious complications such as intestinal tissue damage and hepatic amoebiasis [2,3]. The WHO in its most recent estimates has placed the death toll from amoebiasis at 40,000–100,000 lives annually. The most regularly used clinical drug for the treatment of amoebiasis are derivatives of 5-nitroimidazole such as metronidazole, tinidazole and ornidazole [4–6]. However, the drugs are far from ideal and suffer serious drawbacks. Apart from frequent emergence of resistance, they are associated with several side effects including nausea, vomiting, diarrhoea and gastrointestinal disturbances [2,3,7,8]. Severe side effects include neurological alterations produced by interaction of the drug with the central nervous system and impairment of the cardiac rhythm due to chelation of metronidazole with calcium ions. They are mutagenic in bacteria and carcinogenic in rodents [9–12].

Numerous attempts have been made towards the development of effective and less toxic transition metal ion based antiamoebic agents. Earlier reports from our group includes Pt(II), Pd(II), V(V), Cu(II), Ru(II) and Mo(VI) complexes of thiosemicarbazones, Schiff bases derived from S-alkyldithiocarbazates, pyrazolines or benzimidazole derivatives [13–20]. Continuing our quest, we have synthesized two palladium based complexes of N-(di-alkyl/arylcarbamothioyl)benzamide and tested them for their antiamoebic activity. Similar ligands and their complexes with Ni(II) and Pd(II) have been tested recently by Selvakumaran et al. for their cytotoxic activity [21,22].

Thiourea derivatives have been known for over a century and have vast applications in the field of analytical as well as biological sciences. In transition metal complexes they can function as neutral, monoanionic and dianionic ligands coordinating through O and/or S atoms [23–27]. In addition, these molecules are known to possess antifungal, antitumor, anti-HIV, non-nucleoside inhibitor action of HIV-1 reverse transcriptase, herbicidal, antithyroid, antihelmintic, antibacterial, rodenticidal, insecticidal, plant growth regulator properties and anticancer property [28–36].

2. Experimental

2.1. Materials – instrumentation – physical measurements

All reagents were commercially available and used as received.

* Corresponding author.
E-mail address: rkmanfcy@iitr.ac.in (M.R. Maurya).

http://dx.doi.org/10.1016/j.ejmech.2015.05.006
0223-5234/

The precursor complex $[Pd(DMSO)_2Cl_2]$ [37] and the ligands, N-(dipheylcarbamothioyl)benzamide (HL^1) and N-(di-*n*-butylcarbamothioyl) benzamide (HL^2) [38] were prepared following reported methods. Elemental analysis of the complexes was carried out on an Elementar model Vario-EI-III. The IR spectra were recorded as KBr pellets on a Nicolet 1100 FT-IR spectrometer. Electronic spectra of complexes were recorded in chloroform. ^1H NMR and ^{13}C NMR spectra were recorded in $CDCl_3$ and DMSO-d_6 on a Bruker Avance 500 MHz spectrometer. Thermogravimetric analysis of the complexes was carried out using a Perkin–Elmer (Pyris Diamond) under nitrogen atmosphere.

2.2. Preparations

2.2.1. Synthesis of *cis*–[Pd(L^1–O,S)$_2$] (**1**)

A methanolic solution of the ligand HL^1 (0.664 g, 0.002 mol in 20 mL) was added drop wise to a methanolic solution of $[Pd(DMSO)_2Cl_2]$ (0.334 g, 0.001 mol in 20 mL) at room temperature with stirring. The resulting solution was stirred for 3 h to yield a dark orange precipitate. The precipitate was filtered, washed with cold methanol and dried in *vacuo*. Crystals suitable for x-ray analysis were grown by slow evaporation of dichloromethane solution. Yield: 73%. *Anal*. Calcd. for $C_{40}N_4O_2S_2H_{30}Pd$ (769.24): C, 62.46; H, 3.93; N 7.28; S, 8.34. Found C, 62.4; H, 3.8; N, 7.3; S, 8.3%. IR υ_{max}/cm^{-1}: 1510/1586 (C=N/C=O), 1174 (C=S). λ_{max}/nm (ε/M^{-1} cm^{-1}): 252 (63641), 282 (68930). ^1H NMR (DMSO-d_6)/δ: 7.20–7.70 (m, 30H, ArH).

2.2.2. Synthesis of *cis*–[Pd(L^2–O,S)$_2$] (**2**)

A methanolic solution of the ligand HL^2 (0.584 g, 0.002 mol in 20 mL) was added drop wise to a stirred solution of $[Pd(DMSO)_2Cl_2]$ (0.334 g, 0.001 mol) in 20 mL of methanol and the resulting solution was refluxed for 5 h. After cooling to room temperature, a bright orange precipitate separated which was filtered off, washed with methanol and dried in *vacuo*. Crystals of suitable quality for x-ray analysis were grown by slow evaporation of methanolic solution of **2**. Yield: 80%. *Anal*. Calcd. for $C_{32}H_{46}N_4O_2PdS_2$ (689.28): C, 55.76; H, 6.73; N, 8.13; S, 9.30. Found, C, 55.9; H, 6.7; N, 8.2; S, 9.2%. IR υ_{max}/cm^{-1}: 1513/1586 (C=N/C=O), 1209 (C=S).). λ_{max}/nm (ε/M^{-1} cm^{-1}): 242 (29757), 273 (41924). ^1H NMR (DMSO-d_6)/δ: 0.93, 0.98 (m, 6H each, CH_3), 3.47–3.82 (m, 8H, N–CH_2), 1.39 (m, 8H), 1.68 (m, 4H), 1.75 (m, 4H) (–CH_2–), 7.4 (m, 4H), 7.46–7.50 (m, 2H), 8.23–8.25 (d, 4H) (ArH).

2.3. X-ray crystal structure determination

Three-dimensional X-ray data were collected on a Bruker Kappa Apex CCD diffractometer at room temperature for *cis*–[Pd(L^1–O,S)$_2$] (**1**) and at low temperature for *cis*–[Pd(L^2–O,S)$_2$] (**2**) by the ϕ–ω scan method. Reflections were measured from a hemisphere of data collected from frames each of them covering 0.3° in ω. Of the 54,890 for **1** and 44,411 for **2** reflections were measured, all were corrected for Lorentz and polarization effects and for absorption by multi-scan methods based on symmetry-equivalent and repeated reflections, 7433 and 4926, respectively, independent reflections exceeded the significance level ($|F|/\sigma|F|$) > 4.0. Complex scattering factors were taken from the program package SHELXTL [39]. The structures were solved by direct methods and refined by full matrix least-squares on F^2. Hydrogen atoms were included in calculation positions and refined in the riding mode for **1** and were left to refine freely with isotropic thermal parameters for **2**, except for C(5), C(12), C(16, C(22), C(28) and C(32) which were included in calculation position. Refinements were done with allowance for thermal anisotropy of all non-hydrogen atoms. Further details of the crystal structure determination are given in Table 1. A final difference Fourier map showed no residual density outside: 0.397 and −0.384 e.Å^{-3} for **1** and 1.075 and −0.791 e.Å^{-3} for **2**. A weighting scheme $w = 1/[\sigma^2(F_o^2) + (0.014500\ P)^2 + 1.720900\ P]$ for **1** and $w = 1/[\sigma^2(F_o^2) + (0.038800\ P)^2 + 0.492800\ P]$ for **2**, where $P = (|F_o|^2 + 2|F_c|^2)/3$, were used in the latter stages of refinement.

2.4. Pharmacological screening

2.4.1. In vitro antiamoebic assay

The ligands HL^1 and HL^2 and their palladium complexes *cis*–[Pd(L^1–O,S)$_2$] (**1**) and *cis*–[Pd(L^2–O,S)$_2$] (**2**) were screened *in vitro* for antiamoebic activity against HM1:IMSS strain of *Entamoeba histolytica* by microplate method [40]. All the experiments were carried out in triplicates at each concentration level and repeated thrice. E. histolytica trophozoites were cultured in TYI-S-33 growth medium in wells of 96-well microtiter plates [41]. DMSO (40 μL) was added to all the samples (1 mg) followed by enough culture medium to obtain concentration of 1 mg/mL. The maximum concentration of DMSO in the test did not exceed 0.1%, and at this level no inhibition of amoebal growth had occurred [42]. Compounds were further diluted with medium to a concentration of 0.1 mg/mL. Two fold serial dilutions were made in the wells of 96-well microtiter plate. Each test included metronidazole (MNZ) as the standard amoebicidal drug, control (culture medium plus parasite) and a blank (culture medium only). The cell suspension was then to 10^5 organism/mL by adding fresh medium and 170 μL of this suspension was added to the test and control well in the plate. Plate was sealed and gassed for 10 min with nitrogen before incubation at 37 °C for 72 h. After incubation, the growth of amoebae in the plate was checked with a low power microscope and the optical density of the solution in each well was determined at 490 nm with a microplate reader. The % inhibition of amoebic growth was calculated from the optical densities of the control and test wells and plotted against the logarithm of the dose of the drug tested. Linear regression analysis was used to determine the best-fitted straight line from which the IC_{50} value was found.

2.4.2. Cell viability assay

Cell viability in response to drugs was checked by using MTT assay [43]. Cells (3000 cells/well) were plated in 200 μl DMEM in 96-well plate (flat bottom) in presence of various concentrations of the compounds for different length of time (24 h, 48 h, and 72 h) in a humidified 5% CO_2 incubator at 37 °C. At the end of the stipulated time interval, 20 μl of MTT (5 mg/ml in PBS) solution was added to each well and incubated for 4 h in the 5% CO_2 incubator. After 4 h, medium along with the MTT solution of plates were discarded carefully followed by addition of DMSO (200 μL) in each well. Crystals were dissolved by further incubating the plates for additional 1 h in CO_2 incubator. After 1 h, absorbance was taken in ELISA microplate reader at 570 nm wavelength. Following formula was applied for the calculation of percentage of cell viability (CV):

$$CV = \frac{\text{absorbance of the experimental samples}}{\text{absorbance of the control sample}} \times 100$$

3. Results and discussion

3.1. Synthesis and characterization of complexes

Selvakumaran et al. have reported a series of Pd(II) complexes of the type cis-[Pd(L-O,S)$_2$] with N-(di(alkyl/aryl)carbamothioyl)benzamide ligands (alkyl/aryl = C_2H_5, $(CH_3)_2CHCH_2$, $C_6H_5CH_2$) by reacting $PdCl_2$ with ligands in 1: 2 M ratios [21]. Under these reaction conditions, ligands with alkyl/aryl = C_6H_5 and $CH_3(CH_2)_2CH_2$

Table 1
Crystal data and structure refinement for *cis*–[Pd(L^1–O,S)$_2$] (**1**) and *cis*–[Pd(L^2–O,S)$_2$] (**2**).

	cis–[Pd(L^1–O,S)$_2$] (**1**)	*cis*–[Pd(L^2–O,S)$_2$] (**2**)
Formula	$C_{40}H_{30}N_4O_2PdS_2$	$C_{32}H_{46}N_4O_2PdS_2$
Formula weight	769.20	689.25
T, *K*	293(2)	100(2)
Wavelength, Å	0.71073	0.71073
Crystal system	Triclinic	Triclinic
Space group	$P\bar{1}$	$P\bar{1}$
a/Å	10.0747(12)	9.8422(5)
b/Å	11.2628(14)	10.8823(6)
c/Å	16.5273(19)	15.4682(8)
α/°	105.756(4)	79.634(3)
β/°	91.057(5)	89.073(3)
γ/°	104.412(4)	82.294(4)
V/Å^3	1740.6(4)	1614.92(15)
Z	2	2
F_{000}	784	720
D_{calc}/g cm^{-3}	1.468	1.417
μ/mm^{-1}	0.695	0.739
θ/(°)	1.29 to 28.48	1.34 to 26.37
R_{int}	0.0261	0.1118
Crystal size/mm^3	0.28 × 0.25 × .0.24	0.25 × 0.17 × 0.08
Goodness-of-fit on F^2	1.131	1.058
R_1 [$I > 2\sigma(I)$][a]	0.0335	0.0440
wR_2 (all data)[b]	0.0741	0.1046
Largest differences peak and hole (eÅ^{-3})	0.397 and −0.384	1.075 and −0.791

[a] $R_1 = \sum||F_o| - |F_c||/\sum|F_o|$.
[b] $wR_2 = \{\sum[w(|F_o|^2 - |F_c|^2|)^2]/\sum[w(F_0^4)]\}^{1/2}$.

gave complexes *trans*–[$PdCl_2$(HL–S)$_2$] where only sulphur atom is coordinated. We have isolated complexes of general formula *cis*–[Pd(L–O,S)$_2$] by reacting [Pd(DMSO)$_2$Cl$_2$] with N-(dipheylcarbamothioyl)benzamide (HL^1) and N-(di-*n*-butylcarbamothioyl)benzamide (HL^2) (Eq. (1)) in 1: 2 M ratios. Fig. 1 presents structures of ligands used in the present study and their palladium(II) complexes. These complexes are monomer where ligands behave as monobasic OS bidentate. Complex **1** is soluble only in dichloromethane and sparingly soluble in chloroform while **2** is soluble in methanol, chloroform, dichloromethane, DMF and DMSO

$$[Pd(DMSO)_2Cl_2] + 2H(L{-}O,S) \rightarrow \textit{cis}{-}[Pd(L{-}O,S)_2] + 2DMSO + 2HCl \quad (1)$$

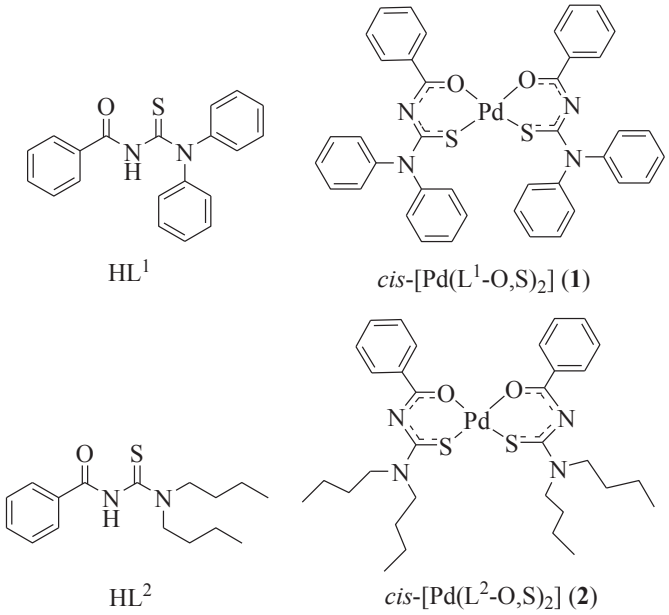

Fig. 1. Structures of ligands and Pd(II) complexes.

[2H(L–O,S) = O,S donor ligands HL^1 and HL^2]

ORTEP diagrams for the compounds *cis*–[Pd(L^1–O,S)$_2$] (**1**) and *cis*–[Pd(L^2–O,S)$_2$] (**2**) are shown in Figs. 2 and 3, respectively. Selected bond distances and angles are given along with the caption of figures and details are given in Table S1 (see supporting information). The complexes adopt a four-coordinated structure in a slightly distorted square planar geometry. The palladium(II) center is coordinated by two O,S-bidentate ligands with a cis-O_2S_2 donor conformation. The ligands act as a thiolate as can be seen from the C–S bond distances in Table S1. Also, there is evidence for elongation of C=O bonds. Associated with this the near planarity of the six-membered chelate rings [mean deviation

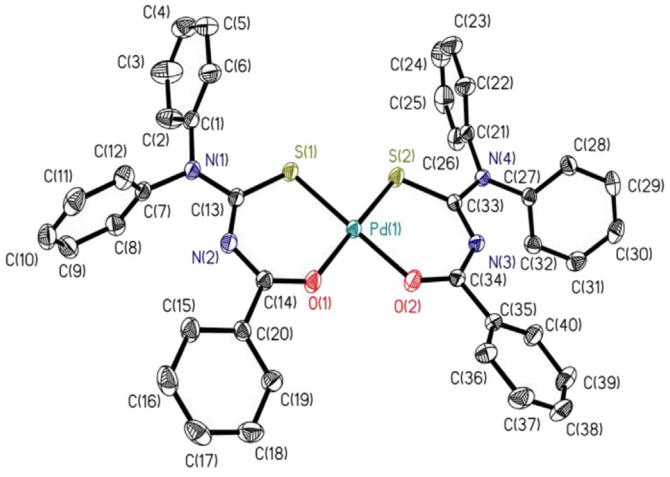

Fig. 2. ORTEP plot of complex *cis*–[Pd(L^1–O,S)$_2$] (**1**). All the non-hydrogen atoms are presented by their 30% probability ellipsoids. Hydrogen atoms are omitted for clarity. Selected bond distances: Pd(1)-O(1) = 2.0252(16) Å, Pd(1)-O(2) = 2.0333(16) Å, Pd(1)-S(1) = 2.2455(6) Å, Pd(1)-S(2) = 2.2371(6) Å, Selected bond angles: O(1)-Pd(1)-O(2) 84.26(6)°, O(1)-Pd(1)-S(2) = 177.55(6)°, O(2)-Pd(1)-S(2) = 94.98(5)°, O(1)-Pd(1)-S(1) = 95.15(5)°, O(2)-Pd(1)-S(1) = 177.86(6)°, S(2)-Pd(1)-S(1) = 85.69(2)°.

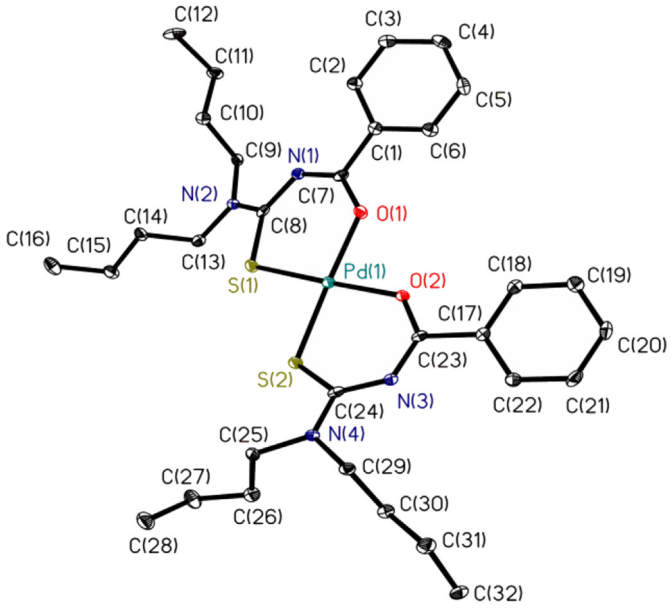

Fig. 3. ORTEP plot of complex *cis*–[Pd(L^2–O,S)$_2$] (**2**). All the non-hydrogen atoms are presented by their 30% probability ellipsoids. Hydrogen atoms are omitted for clarity. Selected bond distances: Pd(1)-O(1) = 2.020(2) Å, Pd(1)-O(2) = 2.017(2) Å, Pd(1)-S(1) = 2.2375(10) Å, Pd(1)-S(2) = 2.2432(10) Å. Selected bond angles: O(1)-Pd(1)-O(2) 84.31(10)°, O(1)-Pd(1)-S(2) = 177.57(7)°, O(2)-Pd(1)-S(2) = 93.28(7)°, O(1)-Pd(1)-S(1) = 93.86(7)°, O(2)-Pd(1)-S(1) = 178.06(8)°, S(2)-Pd(1)-S(1) = 88.54(3)°.

from the planarity = 0.0197(14) for the chelate ring formed by S(1), C(13), N(2), C(14), O(1) and Pd(1), and 0.0126(13) for the chelate ring formed by S(2), C(33), N(3), C(34), O(2) and Pd(1), in *cis*–[Pd(L^1–O,S)$_2$] (**1**) and mean deviation from the planarity = 0.0853(18) for the chelate ring formed by S(1), C(8), N(1), C(7), O(1) and Pd(1), and 0.1072(18) for the chelate ring formed by S(2), C(24), N(3), C(23), O(2) and Pd(1), in *cis*–[Pd(L^2–O,S)$_2$] (**2**) and the distances and equivalence of the C–N bonds, which participate in chelation, see Table S1, suggest significant delocalization of π-electron density over the chelate rings. Angles between chelate rings planes are also close to the ideal value of 0° for a square planar geometry [4.02(8)° in *cis*–[Pd(L^1–O,S)$_2$] (**1**) and 5.39(11)° in *cis*–[Pd(L^2–O,S)$_2$] (**2**). Similar behaviour was found in Ni compounds with similar ligands that have the same geometries and bonds [21,22]. No π–π stacking interactions are found.

Thermogravimetric analysis of the two complexes was carried out between room temperature and 1000 °C with a heating rate of 10 °C/min under nitrogen atmosphere. Both the complexes are stable and do not lose weight up to 200 °C. Further increment of temperature causes decomposition of the complexes in two overlapping steps. The first step ranges from 227 to 375 °C for **1** and 214–364 °C for **2**. The second step completes at ca. 900 °C and 800 °C for **1** and **2**, respectively with the formation of PdS. The observed values of 16.60% for **1** and 19.10% for **2** are close to their theoretical values of 18.00 and 20.18%, respectively. Estimation of the loss of particular fragment of ligands during the whole analysis process has not been possible.

Table 3
In vitro antiamoebic activity of ligands and complexes along with standard against HM1:IMSS strain of *E. histolytica*.

S.No.	Compound	Antiamoebic activity IC_{50} (μM)[a] ± SD[b]
1	HL^1	0.30 ± 0.02
2	HL^2	0.70 ± 0.04
3	*cis*–[Pd(L^1–O,S)$_2$] (**1**)	0.80 ± 0.01
4	*cis*–[Pd(L^2–O,S)$_2$] (**2**)	0.30 ± 0.01
5	Metronidazole	1.40 ± 0.02

[a] The values obtained in at least three separate assays done in triplicate.
[b] Standard Deviation.

The IR spectra of ligands exhibit a strong band at 1652–1690 cm^{-1} and a medium intensity band at 1243–1314 cm^{-1} which are attributed to ν(C=O) and ν(C=S), respectively. A significant shift of both the bands to lower wavenumber strongly suggests the coordination of O and S atoms to the palladium after thioenolization induced delocalization of the electron density [44,45]. This is further supported by the disappearance of a strong band due to the N–H group of free ligands and appearance of a new intense band at ca. 1580 cm^{-1} due to ring ν(C=N) stretch [46] in complexes.

Fig. S1 shows the electronic spectra of the two complexes recorded in chloroform. They exhibit two UV-spectral (ligand) bands at 252 nm (ε = 63,641 M^{-1} cm^{-1}) and 282 nm (ε = 68,930 M^{-1} cm^{-1}) in **1** and at 242 nm (ε = 29,757 M^{-1} cm^{-1}) and 273 nm (ε = 41,924 M^{-1} cm^{-1}) in **2** in the UV region which are similar to other square planar Pd(II) complexes [21,47].

The ^{1}H NMR spectra of HL^2 and *cis*–[Pd(L^2–O,S)$_2$] are given in Fig. S2. The characteristic singlet at 8.81 ppm (in HL^1) and 8.40 ppm (in HL^2) for N–H proton observed in the ligands disappears in the complexes indicating thioenolization followed by delocalization of the electron density associated with the ketonic double bond of the chelate rings (vide supra) [46]. Aromatic protons appear as complex multiplets in **1** while well separated in **2** but they are well within

Table 2
^{13}C NMR spectral data of HL^2 and *cis*–[Pd(L^2–O,S)$_2$] (**2**).

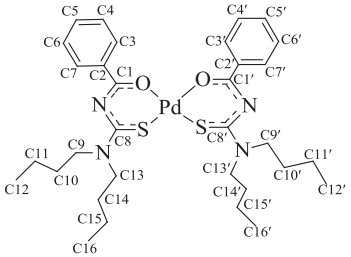

Compound	C1/C1′	C8/C8′	C2/C2′	C3/C3′, C7/C7′	C4/C4′, C6/C6′	C5/C5′	C12/C12′, C16/C16′	C11/C11′, C15/C15′	C10/C10′, C14/C14′	C9/C9′, C13/C13′
HL^2	163.76	179.90	133.00	132.83	127.92	129.00	13.85, 14.01	20.18	28.61,30.26	53.20,53.39
cis–[Pd(L^2–O,S)$_2$] (**2**)	170.46	171.51	137.13	131.43	127.93	129.70	13.88, 13.96	20.29, 20.36	29.55, 30.03	51.67, 52.87

the expected region. The methyl protons of the alkyl chain resonate at 0.89 and 0.97 ppm as two distinct triplets in HL^2 due to their distinct magnetic environments and these bands remain nearly constant in the corresponding complex **2**. The two triplets of methylene protons attached to nitrogen collapse as one multiplet. Similarly, two multiplex of methylene protons of butyl group collapse into one multiplet while other two are well separated as in the ligand. The ^{1}H NMR spectra of both complexes in DMSO-d_6 have also been recorded using freshly prepared solution and 72 h after dissolution, and no change in spectra suggest the stability of these complexes in DMSO.

The ^{13}C NMR spectrum of complex *cis*–[Pd(L^1–O,S)$_2$] (**1**) could not be recorded due to solubility restriction while complex *cis*–[Pd(L^2–O,S)$_2$] (**2**) gave well resolved signals for all carbons in $CDCl_3$. Spectral data of the ligand HL^2 and its complex along with the possible assignments are presented in Table 2 and Fig. S3

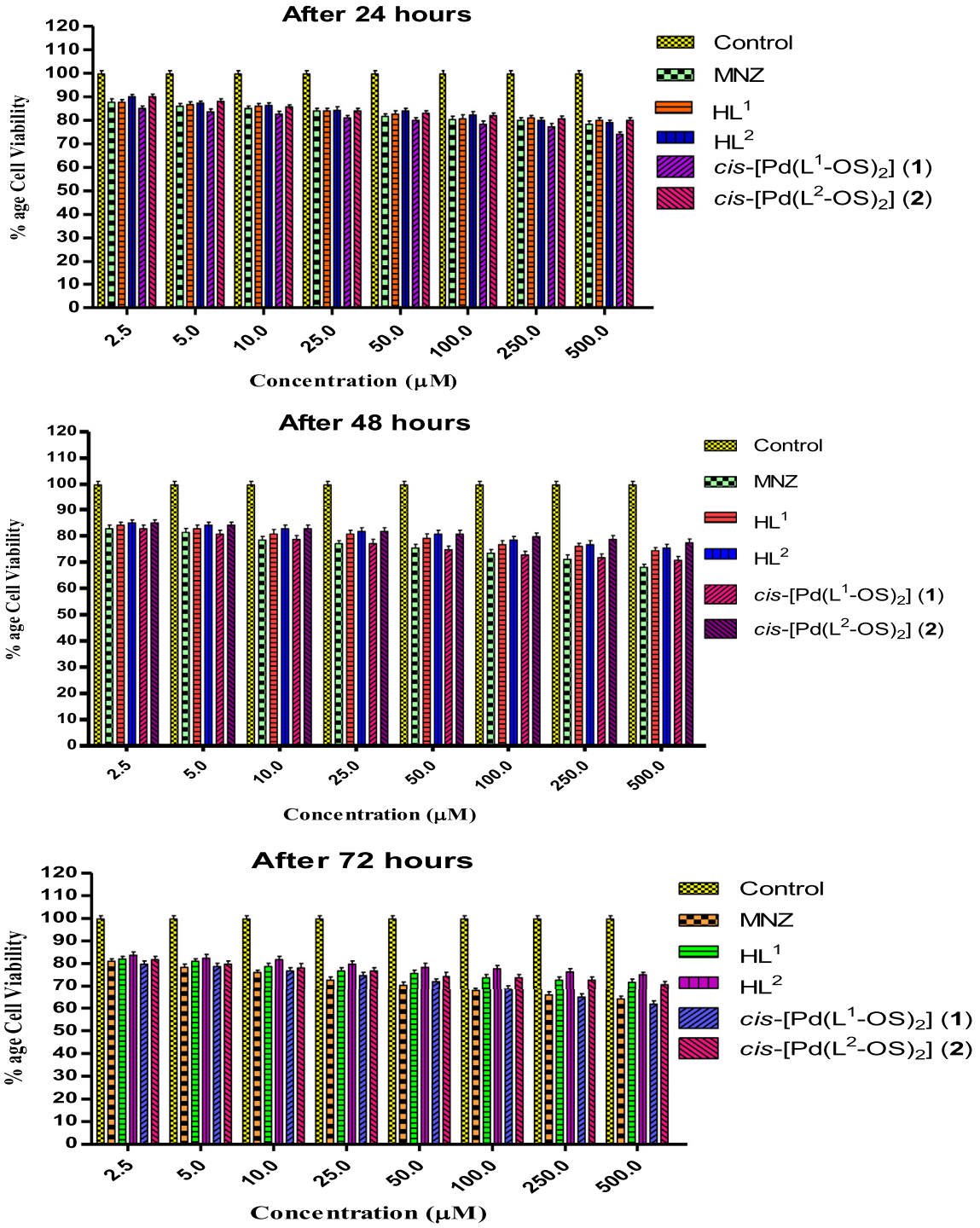

Fig. 4. Assessment of viability of HEK293 Normal cells in response to different compounds. Cells were plated in triplicates for 24 h, 48 h and 72 h and treated with the compounds. Cells treated with DMSO are used as the control. MTT was added after completion of stipulated time intervals and processed. Absorbance was taken at 570 nm. Results were plotted taking control (DMSO) as 100%.

reproduces the spectra of HL^2 and **2**. Assignments of all signals are based on the intensity patterns of the chemical shift and on the coordination-induced shifts [$\delta\Delta = \delta$(complex) − δ(free ligand)] of the signals for carbon atoms in the vicinity of the coordinating atoms [48]. The ligand displays 13 signals corresponding to 16 carbon atoms due to the presence of symmetry in aromatic carbons and alkyl wings. Complex **2** shows two very close signals each for two sets of symmetric pair of carbons C9/C9′ and C13/C13′, C10/C10′, and C14/C14′, C11/C11′ and C15/C15′, and C12/C12′, and C16/C16′ while only one signal for symmetric pair of carbon atoms C2/C2′ to C7/C7′ and even single signal each for C1/C1′ and C8/C8′. A large coordination induced shift of the signal for the carbon atoms bearing the ketonic oxygen (C1/C1′) ($\delta\Delta$ = 6.7 ppm) and the enthiolic sulphur (C8/C8′) ($\delta\Delta$ = −8.39 ppm) atoms demonstrates coordination of these two atoms to the palladium. Carbons closer to the ketonic carbon (i.e. C2/C2′) also register large coordination induced shift and appear at $\delta\Delta$ = 4.13 ppm downfield compared to the free ligand due to adjustment of current.

3.2. Pharmacological screening

3.2.1. Antiamoebic activity

Preliminary experiments were carried out to determine *in vitro* antiamoebic activity of ligands (HL^1 and HL^2) and their palladium complexes {*cis*–[Pd(L^1–O,S)$_2$] (**1**) and *cis*–[Pd(L^2–O,S)$_2$] (**2**)} by microdilution method using HM1:IMSS strain of *Entamoeba histolytica* and their IC_{50} values are reported in Table 3. The antiamoebic effect was compared with the most widely used antiamoebic medication metronidazole which had a 50% inhibitory concentration (IC_{50}) of 1.40 μM in our experiments. The IC_{50} value found for metronidazole is consistent with our previous works, where generally observed IC_{50} value has been found to be below 2.0 μM [13,49]. The results were estimated as the percentage of growth inhibition compared with the untreated controls and plotted as probit values as a function of the drug concentration. IC_{50} and 95% confidence limits were interpolated in the corresponding dose response curve. All the synthesized compounds showed promising antiamoebic activity with IC_{50} values in the range 0.30–0.80 μM as compared to metronidazole as shown in Table 3. The biological data suggests that the complex *cis*–[Pd(L^2–O,S)$_2$] with IC_{50} = 0.30 μM followed a general trend that the biological activity of a compound enhances upon coordination with metal ion. This may be explained by Tweedy's theory [50] where complex **2** showed promising activity than the respective ligand HL^2 (IC_{50} = 0.70 μM). However, the free ligand HL^1 (IC_{50} = 0.30 μM) exhibited better activity than its Pd complex *cis*–[Pd(L^1–O,S)$_2$] (IC_{50} = 0.80 μM) which may be explained considering the lone pair on nitrogen which is in extended conjugation with two phenyl rings which might enhance its activity while the bulky nature of the complex due to the presence of phenyl rings might impose steric hindrance thereby, reducing its efficacy than the corresponding ligand. These two factors plausibly contribute in the increased activity of the ligand HL^1. Thus, in some cases, free ligand does possess higher activity which indicates that the activity does not depend solely on the presence of metal ions but rather a synergistic effect [51]. Further, the stability of these complexes in DMSO for extended period has added advantage but the difference in solubility of these complexes in DMSO also possibly plays some role in their activity but proposing a possible mechanism of action is rather difficult at this stage.

The complex *cis*–[Pd(L^1–O,S)$_2$] was twice as potent as the standard drug and *cis*–[Pd(L^2–O,S)$_2$] presented five times more potency than metronidazole, suggesting the possibility of developing the complexes of general formula *cis*–[Pd(L–O,S)$_2$] with aryl/alkyl = C_6H_5 (HL^1) and $CH_3(CH_2)_2CH_2$ (HL^2) as potential drug candidates for antiamoebic activity.

3.2.2. Cytotoxicity profile: effect of HL^1, HL^2, *cis*–[Pd(L^1–O,S)$_2$] (1) and *cis*–[Pd(L^2–O,S)$_2$] (2) on cell viability of HEK293 cells

To assess the cytotoxic effect of the compounds HL^1, HL^2, *cis*–[Pd(L^1–O,S)$_2$] (**1**) and *cis*–[Pd(L^2–O,S)$_2$] (**2**), HEK293 cells (3000 cells/well) were plated in 96 well tissue culture plates in triplicate. The cells were treated with compounds as indicated in the Fig. 4. The cells were incubated for different time lengths (24 h, 48 h and 72 h) and cell viability assay was performed after completion of the stipulated time intervals. At 48 h all the four synthesised compounds showed good cell viability (80–90%) on HEK293 cells comparable to the standard drug. Slight change was observed in the cell viability after 72 h. The cell viability of *cis*–[Pd(L^1–O,S)$_2$] (**1**) was still comparable to metronidazole, that is more than 70% of the cells were viable whereas for the other three compounds it was 80–90% cell viability. Both the ligands and the complexes showed better cell viability hence can be considered less toxic.

4. Conclusions

Two palladium(II) compounds having the general formula, *cis*–[Pd(L-O,S)$_2$] with ligand N-(di(butyl/phenyl)carbamothioyl)benzamide have been prepared where two monobasic OS donor ligands coordinate to palladium in a cis-O_2S_2 conformation. The two ligands and their Pd(II) complexes have been screened for their *in vitro* antiamoebic activity against HM1:IMSS strain of *Entamoeba histolytica* and for their *in vitro* cytotoxic activity against HEK293 cells. Ligands as well as complexes both showed excellent activity against *E. histolytic*a with the observed IC_{50} values being significantly lower than that of metronidazole. In fact complex *cis*–[Pd(L^2–O,S)$_2$] presents five times more potency than metronidazole, suggesting the possibility of developing the complexes of general formula *cis*–[Pd(L–O,S)$_2$] as potential drug candidates for antiamoebic activity. All four synthesised compounds showed good cell viability, hence they are less toxic.

Acknowledgement

BU is thankful to Indian Institute of Technology Roorkee, Roorkee for MHRD fellowship.

Appendix A. Supplementary data

Supplementary data related to this article can be found at http://dx.doi.org/10.1016/j.ejmech.2015.05.006.

References

[1] K.S. Ralston, W.A. Petri, The ways of a killer: how does *Entamoeba histolytica* elicit host cell death? Essays Biochem. 51 (2011) 193–210.
[2] S. Marion, N. Guillen, Genomic and proteomic approaches highlight phagocytosis of living and apoptotic human cells by the parasite *E. histolytica*, Int. J. Parasitol. 36 (2006) 131–139.
[3] S.L. Stanley Jr., Amoebiasis, Lancet 361 (2003) 1025–1034.
[4] D.I. Edwards, Nitroimidazole drugs–action and resistance mechanisms. II. Mechanisms of resistance, J. Antimicrob. Chemother. 31 (1993) 201–210.
[5] M.M.L. Nigro, A.B. Gadano, M.A. Carballo, Evaluation of genetic damage induced by a nitroimidazole derivative in human lymphocytes: tinidazole (TNZ), Toxicol. Vitro 15 (2001) 209–213.
[6] N.J. Moreno, R. Docampo, Mechanism of toxicity of nitro compounds used in the chemotherapy of trichomoniasis, Environ. Health Perspect. 64 (1985) 199–208.
[7] D. Gambino, Potentiality of vanadium compounds as anti-parasitic agents, Coord. Chem. Rev. 255 (2011) 2193–2203.
[8] K. Hounkong, N. Sawangjaroen, W. Kongyen, V. Rukachaisiriku, S.P. Voravuthikunchai, S. Phongpaichit, Anti-intestinal protozoan activities of 1-hydroxy-2-hydroxymethylanthraquinone from *Coptosapelta flavescens*, Asian. Pac. J. Trop. Dis. 4 (2014) 457–462.
[9] Y. Akgun, I.H. Tacyldz, Y. Celik, Amoebic liver abscess: changing trends over 20 years, World J. Surg. 23 (1999) 102–106.
[10] A. Sadowska, S. Prokopiuk, W. Miltyk, A. Surażyński, J. Konończuk, D. Sawicka,

H. Car, Metronidazole affects breast cancer cell lines, Adv. Med. Sci. 58 (2013) 90–95.
[11] K.B. Caylor, M.K. Cassimatis, Metronidazole neurotoxicosis in two cats, J. Am. Anim. Hosp. Assoc. 37 (2001) 258–262.
[12] K. Kapoor, M. Chandra, D. Nag, J.K. Paliwal, R.C. Gupta, R.C. Saxena, Evaluation of metronidazole toxicity: a prospective study, Int. J. Clin. Pharmacol. Res. 19 (1999) 83–88.
[13] N. Bharti, Shailendra, M.T.G. Garza, D.E.C. Vega, J.C. Garza, K. Saleem, F. Naqvia, M.R. Maurya, A. Azam, Synthesis, characterization and antiamoebic activity of benzimidazole derivatives and their vanadium and molybdenum complexes, Bioorg. Med. Chem. Lett. 12 (2002) 869–871.
[14] M.R. Maurya, S. Khurana, Shailendra, A. Azam, W. Zhang, D. Rehder, Synthesis, characterisation and antiamoebic studies of dioxovanadium(V) complexes containing ONS donor ligands derived from *S*-benzyldithiocarbazate, Eur. J. Inorg. Chem. (2003) 1966–1973.
[15] N. Bharti, F. Athar, M.R. Maurya, A. Azam, Synthesis, characterization and in vitro anti-amoebic activity of new palladium(II) complexes with 5-nitrothiophene-2-carboxaldehyde N(4)-substituted thiosemicarbazones, Bioorg. Med. Chem. 12 (2004) 4679–4684.
[16] M.R. Maurya, A. Kumar, A.R. Bhat, A. Azam, C. Bader, D. Rehder, Dioxo- and oxovanadium(V) complexes of thiohydrazone ONS donor ligands: synthesis, characterization, reactivity, and antiamoebic activity, Inorg. Chem. 45 (2006) 1260–1269.
[17] S. Singh, F. Athar, M.R. Maurya, A. Azam, Cyclooctadiene Ru(II) complexes of thiophene-2-carboxaldehyde-derived thiosemicarbazones: synthesis, characterization and antiamoebic activity, Eur. J. Med. Chem. 41 (2006) 592–598.
[18] M.R. Maurya, A. Kumar, M. Abid, A. Azam, Dioxovanadium(V) and μ-oxo bis [oxovanadium(V)] complexes containing thiosemicarbazone based ONS donor set and their antiamoebic activity, Inorg. Chim. Acta 359 (2006) 2439–2447.
[19] M.R. Maurya, S. Agarwal, M. Abid, A. Azam, C. Bader, M. Ebel, D. Rehder, Synthesis, characterisation, reactivity and *in vitro* antiamoebic activity of hydrazone based oxovanadium(IV), oxovanadium(V) and μ-bis(oxo)bis{oxovanadium(V)} complexes, Dalton Trans. (2006) 937–947.
[20] M.R. Maurya, A.A. Khan, A. Azam, S. Ranjan, N. Mondal, A. Kumar, F. Avecilla, J.C. Pessoa, Vanadium complexes having $[V^{IV}O]^{2+}$ and $[V^{V}O_2]^{+}$ cores with binucleating dibasic tetradentate ligands: synthesis, characterization, catalytic and antiamoebic activities, Dalton Trans. 39 (2010) 1345–1360.
[21] N. Selvakumaran, S. Weng Ng, E.R.T. Tiekink, R. Karvembu, Versatile coordination behavior of *N*,*N*-di(alkyl/aryl)-*N*′-benzoylthiourea ligands: synthesis, crystal structure and cytotoxicity of palladium(II) complexes, Inorg. Chim. Acta 376 (2011) 278–284.
[22] N. Selvakumaran, A. Pratheepkumar, S.W. Ng, E. Tiekink, R. Karvembu, Synthesis, structural characterization and cytotoxicity of nickel(II) complexes containing 3,3-dialkyl/aryl-1-benzoylthiourea ligands, Inorg. Chim. Acta 404 (2013) 82–87.
[23] C.K. Ozer, H. Arslan, D. Vanderveer, G. Binzet, Synthesis and characterization of *N* -(alky(aryl)carbamothioyl)cyclohexanecarboxamide derivatives and their Ni(II) and Cu(II) complexes, J. Coord. Chem. 62 (2009) 266–276.
[24] H. Arslan, N. Kulcu, U. Florke, Normal coordinate analysis and crystal structure of *N*,*N*-dimethyl-*N*′-(2-chloro-benzoyl)thiourea, Spectrochim. Acta Part A 64 (2006) 1065–1071.
[25] N. Gunasekaran, P. Ramesh, M.N.G. Ponnuswamy, R. Karvembu, Monodentate coordination of *N*-[di(phenyl/ethyl)carbamothioyl]benzamide ligands: synthesis, crystal structure and catalytic oxidation property of Cu(I) complexes, Dalton Trans. 40 (2011) 12519–12526.
[26] N. Gunasekaran, R. Karvembu, Synthesis, characterization, and catalytic applications of Ru(III) complexes containing *N*-[di(alkyl/aryl)carbamothioyl] benzamide derivatives and triphenylphosphine/triphenylarsine, Inorg. Chem. Commun. 13 (2010) 952–955.
[27] E.R. Fernández, E. García, M.R. Hermosa, A.J. Sánchez, M.M. Sánchez, E. Monte, J.J. Criado, Chloride and ethyl ester morpholine thiourea derivatives and their Ni(II) complexes. Crystal and molecular structures of the thiourea derivativeL-leucine methyl ester and its complexes with Cu(II) and Pt(II). Growth of the pathogenic fungus *Botrytis cinerea*, J. Inorg. Biochem. 75 (1999) 181–188.
[28] C. Sacht, M.S. Datt, Synthesis and characterisation of mixed-ligand platinum(II) –sulfoxide complexes, [PtCl(DMSO)(L)], for potential use as chemotherapeutic agents (HL=*N*,*N*-dialkyl-*N*′-(3-*R*-benzoyl)thiourea), Polyhedron 19 (2000) 1347–1354.
[29] M. Domínguez, E. Anticó, L. Beyer, A. Aguirre, S.G. Granda, V. Salvadó, Liquid–liquid extraction of palladium(II) and gold(III) with *N*-benzoyl-*N*′,*N*′-diethylthiourea and the synthesis of a palladium benzoylthiourea complex, Polyhedron 21 (2002) 1429–1437.
[30] R. del Campo, J.J. Criado, R. Gheorghe, F.J. González, M.R. Hermosa, F. Sanz, J.L. Manzano, E. Monte, E.R. Fernández, *N*-benzoyl-*N*′-alkylthioureas and their complexes with Ni(II), Co(III) and Pt(II) – crystal structure of 3-benzoyl-1-butyl-1-methyl-thiourea: activity against fungi and yeast, J. Inorg. Biochem. 98 (2004) 1307–1314.
[31] W. Hermindez, E. Spodine, L. Beyer, U. Schrtider, R. Richter, J. Ferreira, M. Pavani, Synthesis, characterization and antitumor activity of copper(II) complexes, $[CuL_2]$ [HL^{1-3} =N,N-Diethyl-N′-(R-Benzoyl)thiourea (R=H, o-Cl and p-NO_2)], Bioinorg. Chem. Appl. 3 (2005) 299–316.
[32] M.K. Rauf, Imtiaz-ud-Din, A. Badshah, M. Gielen, M. Ebihara, D. de Vos, S. Ahmed, Synthesis, structural characterization and *in vitro* cytotoxicity and anti-bacterial activity of some copper(I) complexes with N,N′-disubstituted thioureas, J. Inorg. Biochem. 103 (2009) 1135–1144.
[33] H. Arslan, N. Duran, G. Borekci, C.K. Ozer, C. Akbay, Antimicrobial activity of some thiourea derivatives and their nickel and copper complexes, Molecules 14 (2009) 519–527.
[34] C. Limban, L. Marutescu, M.C. Chifiriuc, Synthesis, spectroscopic properties and antipathogenic activity of new thiourea derivatives, Molecules 16 (2011) 7593–7607.
[35] M. Kalhor, M. Salehifar, I. Nikokar, Synthesis, characterization, and antibacterial activities of some novel N,N′-disubstituted thiourea, 2-amino thiazole, and imidazole-2-thione derivatives, Med. Chem. Res. 23 (2014) 2947–2954.
[36] N. Bharti, M.R. Maurya, F. Naqvia, A. Azam, Synthesis and antiamoebic activity of new cyclooctadiene ruthenium(II) complexes with 2-acetylpyridine and benzimidazole derivatives, Bioorg. Med. Chem. Lett. 10 (2000) 2243–2245.
[37] J.H. Price, A.N. Williamson, R.F. Schramm, B.B. Wayland, Palladium(II) and platinum(II) alkyl sulfoxide complexes. Examples of sulfur-bonded, mixed sulfur- and oxygen-bonded, and totally oxygen-bonded complexes, Inorg. Chem. 116 (1972) 1280–1284.
[38] H. Arslan, N. Kulcu, U. Florke, Synthesis and characterization of copper(II), nickel(II) and cobalt(II) complexes with novel thiourea derivatives, Trans. Met. Chem. 28 (2003) 816–819.
[39] G.M. Sheldrick, SHELXL-97: an Integrated System for Solving and Refining Crystal Structures from Diffraction Data (Revision 4.1), University of Göttingen, Germany, 1997.
[40] C.W. Wright, M.J. O'Neill, J.D. Phillipson, D.C. Warhurst, Use of microdilution to assess in vitro antiamoebic activities of Brucea javanica fruits, Simarouba amara stem, and a number of quassinoids, Antimicrob. Agents Chemother. 32 (1988) 1725–1729.
[41] A.T. Keene, A. Harris, J.D. Phillipson, D.C. Warhurst, In vitro amoebicidal of natural products; part I. methodology, Planta Med. 52 (1986) 278–284.
[42] F.D. Gillin, D.S. Reiner, M. Suffness, Bruceantin, a potent amoebicide from a plant, *Brucea antidysenterica*, Antimicrob. Agents Chemother. 22 (1982) 342–345.
[43] T. Mosmann, Rapid colorimetric assay for cellular growth and survival: application to proliferation and cytotoxicity assays, J. Immun. Methods 65 (1983) 55–63.
[44] Z. Weiqun, Y. Wen, X. Liqun, C. Xianchen, *N*-Benzoyl-*N*′-dialkylthiourea derivatives and their Co(III) complexes: structure, and antifungal, J. Inorg. Biochem. 99 (2005) 1314–1319.
[45] N. Gunasekaran, P. Jerome, S.W. Ng, E.R.T. Tiekink, R. Karvembu, *Tris*-chelate complexes of cobalt(III) with *N*-[di(alkyl/aryl)carbamothioyl] benzamide derivatives: synthesis, crystallography and catalytic activity in TBHP oxidation of alcohols, J. Mol. Catal. A Chem. 353–354 (2012) 156–162.
[46] G. Binzet, N. Kulcu, U. Florke, H. Arslan, Synthesis and characterization of Cu(II) and Ni(II) complexes of some 4-bromo- *N* -(di(alkyl/aryl)carbamothioyl) benzamide derivatives, J. Coord. Chem. 62 (2009) 3454–3462.
[47] I.P. Romm, A.A. Malkov, S.A. Lebedev, V.V. Levashova, T.M. Buslaeva, The electronic spectra and structure of palladium(II) molecular complexes and clusters, Russ. J. Phys. Chem. A 85 (2011) 248–253.
[48] A.D. Keramidas, A.B. Papaioannou, A. Vlahos, T.A. Kabanos, G. Bonas, A. Makriyannis, C.P. Raptopoulou, A. Terzis, Model investigations for vanadium–protein interactions. Synthetic, structural, and physical studies of vanadium(III) and oxovanadium(IV/V) complexes with amidate ligands, Inorg. Chem. 35 (1996) 357–367.
[49] S. Singh, N. Bharti, F. Naqvi, A. Azam, Synthesis, characterization and in vitro antiamoebic activity of 5-nitrothiophene-2-carboxaldehyde thiosemicarbazones and their Palladium (II) and Ruthenium (II) Complexes, Eur. J. Med. Chem. 39 (2004) 459–465.
[50] B.G. Tweedy, Plant extracts with metal ions as potential antimicrobial agents, Phytopathology 55 (1964) 910–917.
[51] A.O. Sobola, G.M. Watkins, B. Van Brecht, Synthesis, characterization and antimicrobial activity of copper(II) complexes of some ortho-substituted aniline Schiff bases; crystal structure of bis(2-methoxy-6-imino)methylphenol copper(II) complex, S. Afr. J. Chem. 67 (2014) 45–51.